Reviewer 1

In the manuscript titled *Molecular dynamics study on the liquid-liquid contact angle in liquid-liquid phase separated aerosols* Zhang et. al. present MD-simulation-based calculations of the liquid-liquid contact angles in partially engulfed liquid-liquid phase separated (LLPS) aerosol. Indeed, the particle morphology, as well as the partitioning of components can drastically impact aerosol growth kinetics, therefore knowing the morphology of nanoparticles, whose size falls below the experimentally accessible size range is important and timely. The choice of molecular dynamics as a method to estimate contact angles and particle morphology is also appropriate. Therefore, the paper could represent a significant contribution to our understanding of LLPS aerosol, however, to be publishable in ACP, some major concerns need to be addressed.

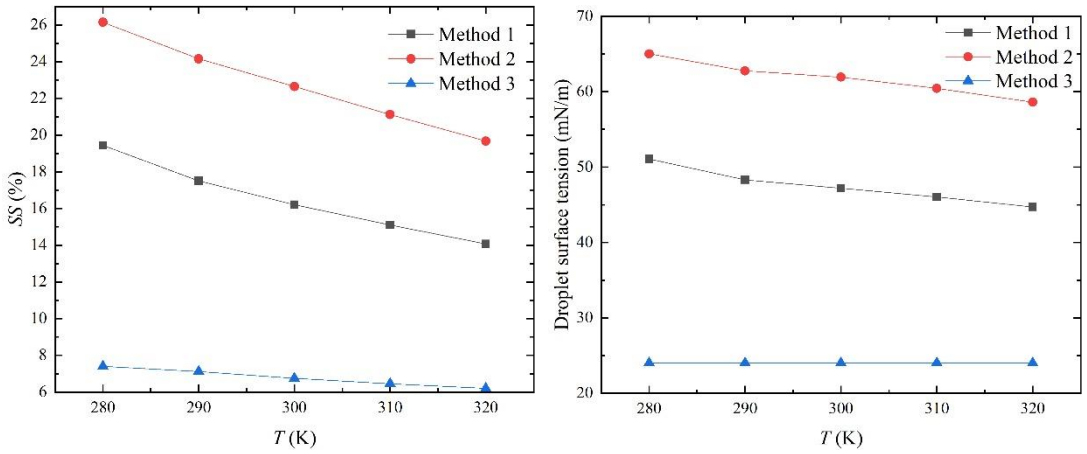
I. Major revision items:

I.1) In its current format the paper provides detailed a phenomenological description of the impact of temperature, concentration of multiple atmospherically relevant components (salts, water, organic acids and alkanes), and retrieval method on the contact angle in LLPS droplets. However, it only marginally mentions atmospheric impacts and does not provide any quantitative analysis of how these results affect main properties needed to describe growth kinetics or aerosol thermodynamics. I believe that ACP's focus is on atmospheric science and therefore a direct link between the MD data and for instance estimated growth timescales, water uptake kinetics, Kohler curves etc. would significantly improve the fit of this manuscript to the journal's scope. Please add model calculations (e.g. gas to particle partitioning) that link the phenomenological description to atmospheric impacts.

Answer: Thank you very much for this valuable comment. In the revised manuscript, the saturated vapor pressure of water on the surface of a droplet and the condensation rate of water on the surface of the droplet are investigated. The revisions added to the

revised manuscript are listed below.

To provide quantitative evidence, the water vapor supersaturations SS/[100%] = *S*-1 of droplet composed of 8000 water, 2000 dodecane and 100 NaCl at various temperatures (280 K, 290 K, 300 K, 310 K, and 320 K) have been calculated by Köhler theory using E-AIM derived water activities and three different description methods of surface tension. In Method 1, the droplet surface tension is calculated based on the surface-area-weighted mean of the surface tensions from NaCl solution phase and dodecane phase together with the contact angle reported in Fig. 5(b). In Method 2, surface tension of the NaCl solution droplet derived from E-AIM model is used. In Method 3, it is assumed that dodecane completely envelops the sodium chloride solution droplet in shell form, and the surface tension of the droplet is equal to that of squalane. Comparison of *SS* and the corresponding surface tension are presented in Fig. 11. It can be observed from Fig. 11(a) that at all temperatures the results of *SS* using different methods satisfy the following order: Method 2 > Method 1 > Method 3. It can be explained by the consistent order of droplet surface tension shown in Fig. 11(b).



(a) (b)

Fig. 11 Comparison of *SS* of 8000 water - 2000 dodecane - 100 NaCl droplet at

various temperatures (280, 290, 300, 310, 320 K) calculated based on three different description methods of surface tension (a) and the corresponding surface tension (b)

(***shown in lines 546 ~ 564 , pages 30-31 in the revised manuscript***)

A case study was implemented to compare the effects of different surface accommodation coefficients on droplet condensation process. The condensation rates of the droplet composed of 8000 water, 2000 dodecane and 100 NaCl at various temperatures (280 K, 290 K, 300 K, 310 K and 320 K) under a water vapor saturation of S = 1.6 were calculated based on the Kumala model (Kulmala et al., 1993) with two different mass (heat) accommodation coefficients (λ_M and λ_T). In the first scenario, both mass and heat accommodation coefficients were calculated using the corresponding contact angle (Fig. 5(b)) (Model S1), while they are set to 1 in the second scenario (Model S2). Details of the Kumala model are presented in the Supplement. The condensation rates (dr/dt) and the mass (heat) accommodation coefficients (λ_M and λ_T) at the initial time based on two models are presented in Fig. 12.

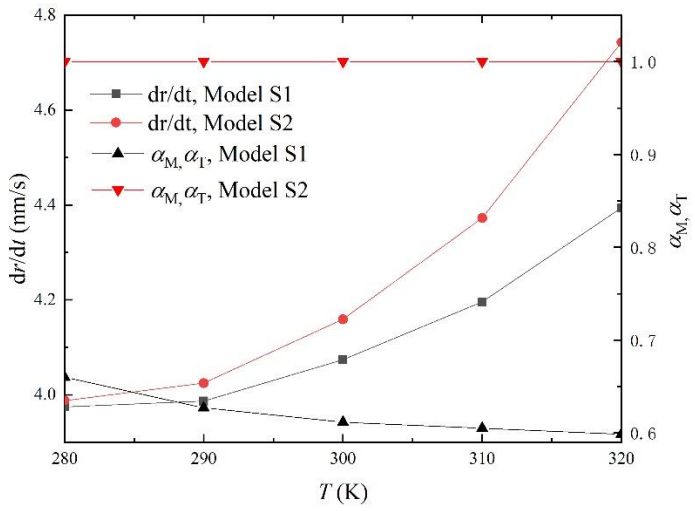


Fig. 12 The theoretical condensation rates (dr/dt) the mass (heat) accommodation

coefficients (λ_M and λ_T) at the initial time of the droplet composed of 8000 water, 2000 dodecane and 100 NaCl at various temperatures (280 K, 290 K, 300 K, 310 K and 320 K) under a water vapor saturation of S = 1.6

As shown in Fig. 12, compared with Model S2, calculating the mass (heat) accommodation coefficients from the contact angle leads to a considerable reduction in droplet condensation rate. This study provides ideas for the quantitative description of contact angle, and in the future, the calculation method of contact angle can be improved through the study of LLPS particles with various components and sizes. (***shown in lines 594 ~ 618, pages 33-34 in the revised manuscript***)

4. Details of the Kumala model

In the Kumala model (Kulmala et al., 1993), the mass flux (I) of water on the droplet surface during condensation can be calculated by

$$I = -4\pi\rho r^2 \frac{\mathrm{d}r}{\mathrm{d}t} = -4\pi r\left(S - a_w\right)\left[\frac{RT_g}{\beta_M M_w D_g P\left(T_g\right) A} + \frac{a_w M_w L_w^2}{\beta_T R K\left(T_g\right) T^2}\right]^{-1} \quad (5)$$

where r is the radius of the droplet, S is the saturation ratio of water vapor in the gas phase, a_w is the water activity of the droplet, R is the gas constant, T_g is the gas phase temperature far from the droplet, ρ_w, M_w and L_W are the density, the molar mass and the latent heat of water, $K(T_g)$ is the thermal conductivity of the carrier gas, A is the Stefan flow correction factor, D_g is the gas-phase diffusion coefficient of water, $P(T_g)$ is the saturated vapor pressure of the water, and β_M and β_T are the transitional correction factors for mass and heat transfer accounting for the different Kn regimes, respectively. Fuchs−Sutugin transitional correction factors are used in the Kulmala model:

$$\beta_{ii} = \frac{1 + Kn_{ii}}{1 + \left(\frac{4}{3\alpha_{ii}} + 0.377 \right) Kn_{ii} + \frac{4}{3\alpha_{ii}} Kn_{ii}^2} \tag{6}$$

where Kn_{ii} and α_{ii} are the Knudsen number for either mass (ii = M) or heat (ii = T) transfer, and the mass (ii = M) or thermal (ii = T) accommodation coefficients, respectively. Kn_{M} and Kn_{T} are given by

$$Kn_{\mathrm{M}} = \frac{\lambda_{\mathrm{M}}}{r} = \frac{3D_g}{\bar{c}r} \tag{7}$$

$$Kn_{\mathrm{T}} = \frac{\lambda_{\mathrm{T}}}{r} = \frac{3K}{\rho C_v \bar{c} r} \tag{8}$$

where λ_{M} and λ_{T} are the effective mean free paths for the mass transfer and heat transfer, respectively, C_{V} is the specific heat capacity of the gas, $\bar{c}$ is the average mean speed of the gas molecules.

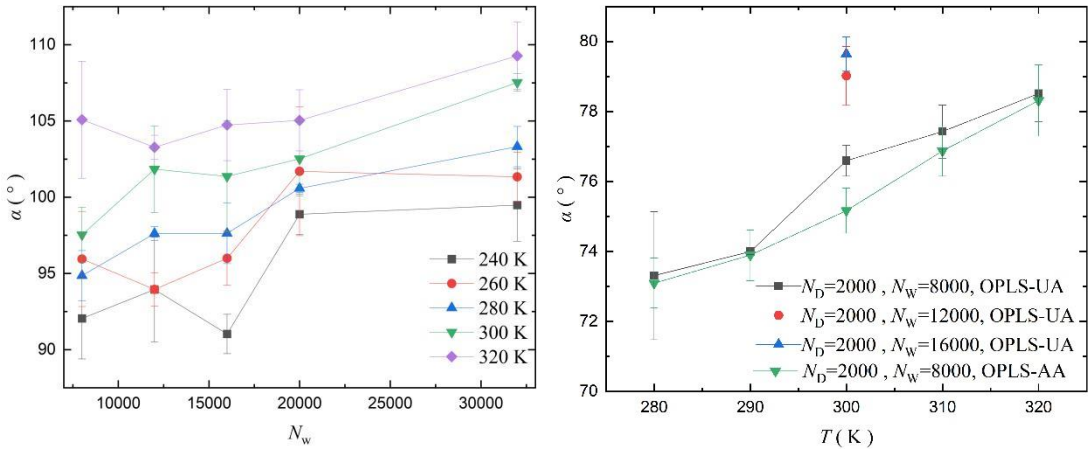
(***shown in lines 150 ~ 170 , page 11 in the supplement file***)

I.2) I am concerned about the use of two relatively outdated coarse grained potentials. The OPLS-UA appears to be justified for aqueous system, and indeed it has the SPC/E water which is atomistic, even though it is known to have some discrepancies which might impact current calculations. In particular the liquid phase tends to retain unphysical planar molecular structures which may impact the surface tension calculations and the interfacial structure between the polar and the non-polar phases. The Martini forcefield, on the other hand, is extremely problematic: its water representation consists of a bead which collectively represents 4 water molecules, which definitely impacts pressure tensors as well as interfacial structures. Further, as the authors also realise it shows artificial phase separation and really low surface tension values (much below the experimental value), which is expected due to the number of water beads' impact on the pressure tensors. Based on the limitations of both models, I suggest the authors to remove

the Martini forcefield and compare the OPLS-UA with a more up-to-date atomistic potential (e.g. OPLS-AA with SPC/E, CHARMM or AMBER with TIP4P or TIP5P).

Answer: Thank you very much for this valuable comment. I fully agree with the reviewer's observation on the limitations of the OPLS-UA and the Martini molecular force-field parameters used herein.

Following the reviewer's suggestion, we adopt the OPLS-AA all-atom force field to calculate the contact angle of binary water (N_W = 8000)-dodecane (N_D = 2000) droplets at difference temperatures, so as to evaluate the accuracy of the Martini and OPLS-UA force field parameters. The corresponding results are shown in Fig. 3. It can be observed from Fig. 3(b) that the contact values calculated by the OPLS-AA force filed are in good agreement with those from the OPLS-UA force field. However, results of the Martini force field are significantly greater than those of the UA force field.



(a) (b)

Fig. 3 Contact angles of water-dodecane droplets under different temperature and water content conditions. (a) Results of Martini force field (N_D = 2000), and (b) results of OPLS-UA and OPLS-AA force field

The significant difference between the Martini molecular force field results and experimental results in describing the surface tension of pure water is consistent with existing literature. The improved versions of the Martini force field (Marrink et al., 2007; Souza et al., 2021) have failed to address this issue. In this study, we found that the Martini force field overestimates the contact angle of liquid-liquid phase separation

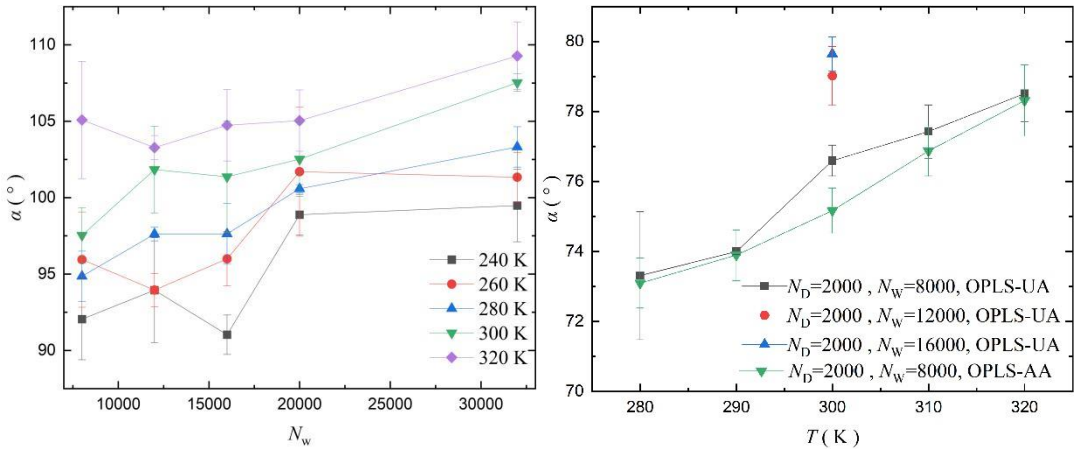
particles. However, the Martini force field can qualitatively describe the influence of temperature and water molecule content on contact angle. Moreover, the coarse-grained Martini force field plays an important role in the study of aerosol droplet structure and interface parameters due to a significant increase in computational efficiency, especially in the study of particle size effects. Therefore, the contact angle and interfacial tension results based on the Martini force field are retained in the revised manuscript, and the shortcomings and advantages of Martini force field are discussed in detail

The revisions in the revised manuscript are listed below.

The contact angles predicted by the Martini force field are larger than those from the OPLS-UA force field, while the OPLS-UA force field yields contact angles close to those of the OPLS-AA force field. In addition, the Martini force field captures a stronger effect of NaCl on the contact angle compared with the OPLS-UA force field.

(***shown in lines 31 ~ 34, pages 1 in the Abstract section of the revised manuscript***)

Based on the qualitative description, we further studied the mechanisms of temperature and water content on the liquid-liquid contact angle of the water-dodecane binary droplet, using the contact angle calculation method described in Section 2.2. Corresponding results are shown in Fig. 3, in which outcomes based on both the Martini force field and the OPLS-UA force field are included. To evaluate the accuracy of the Martini force field and the OPLS-UA force field parameters, the contact angles of binary water (N_W = 8000)-dodecane (N_D = 2000) droplets at difference temperatures based on the OPLS-AA all-atom force field (Jorgensen et al., 1996) are also presented.



(a) (b)

Fig. 3 Contact angles of water-dodecane droplets under different temperature and water content conditions. (a) Results of the Martini force field (N_D = 2000), and (b) results of the OPLS-UA force field and the OPLS-AA force field

As shown in Fig. 3(a), when the temperature is constant, the contact angle is positively correlated with the number of water molecules, which is consistent with the qualitative results obtained from Fig. 2. In addition, when the content of water molecules in the droplet is the same, the contact angle shows an increasing trend with the increase of temperature. This result is consistent with the variation of the contact angle between nonane and water with temperature in Obeidat et al. (2015). It can be seen from Fig. 3(b) that the contact angle obtained based on the OPLS-UA force field is positively correlated with both temperature and water molecule content, which is consistent with the result based on the Martini force field. The mechanism of temperature's effect on contact angle will be discussed in the Discussions section (Section 3.5), taking into account the results of changes in interfacial tension. Fig. 3(b) also indicates that the contact values calculated by the OPLS-AA force filed are in good agreement with those from the OPLS-UA force field. However, results of the Martini

force field are significantly greater than those of the UA force field.

(*shown in lines 217 ~ 244, pages 11 -12 in the revised manuscript*)

The Martini force field parameters have limitations in describing the surface tension of pure water and therefore the water-dodecane contact angle. The core problem of the Martini force field lies in the compromises inherent in its coarse-grained design: representing multiple water molecules with a single bead eliminates orientational degrees of freedom and hydrogen-bond directionality, yet water's surface tension arises precisely from the anisotropic net attraction caused by surface molecules being unable to form a complete hydrogen-bonding network. Meanwhile, in Martini force field each water bead is modeled as a simple 12-6 Lennard-Jones particle, and its nonbonded parameters are optimized for bulk-phase partitioning free energies. Because such a simplified LJ potential is known to overly stabilize the solid phase and cause unphysical freezing at elevated temperatures, the force field deliberately avoids using surface tension as a fitting target. Consequently, its water beads lack explicit hydrogen bonding and electrostatics, causing the predicted surface tension of pure water to be only about one-third of the experimental value (Iannetti et al., 2024). Nevertheless, despite these limitations in quantitatively reproducing interfacial properties, The Martini force field remains a highly efficient coarse-grained model, valuable for investigating qualitative mechanisms underlying how microscopic parameters modulate interfacial behavior, especially for exploring particle size effects.

(*shown in lines 601 ~ 618 , page 34 in the revised manuscript*)

The Martini force field generally yields larger contact angles than the OPLS-UA force field, whereas contact angles predicted by OPLS-UA are comparable to those obtained with the OPLS-AA force field.

(***shown in lines 625 ~ 627 , page 35 in the revised manuscript***)

II. Minor revision items:

II.1) Please add more information about the MD simulations in the methods section of the main text. (Temperatures, type of thermostat, barostat if applicable, type of long-range treatment, software used, length of equilibration and production, how was equilibration monitored, how were the systems prepared).

Answer: Thank you very much for this valuable comment. The added content is as follows.

Moltemplate was used to establish the initial droplet models. The initial configuration contained two tangential clusters: one cluster was water (or water mixed with sodium chloride or suberic acid), and the other was pure dodecane. The system firstly underwent pre-equilibration for 2 ns at 240 K, then was heated to the target temperature for subsequent equilibrium runs. The interaction energy between the two clusters was monitored to assess whether the system reached equilibrium during pre-equilibration. In the simulations based on the Martini force field, non-bonded interactions were truncated at a distance of r_c = 1.2 nm. In the united-atom OPLS-UA force field simulations, the LJ interaction cutoff distance was set to 1.4 nm, and the PPPM method was used to calculate the long-range Coulombic interactions. The interactions between different atoms in the force field were calculated using the Lorenz-Berthelot (LB) combination rule 41, where $\varepsilon_{ij} = (\varepsilon_i\varepsilon_j)^{1/2}$ and $\sigma_{ij} = (\sigma_i + \sigma_j)/2$. The time step was set to 5 fs, and the SHAKE algorithm was used to fix the bond angles and bond lengths of SPC/E water. The simulation process adopted the NVT ensemble, and the temperature was controlled by the Nose-Hoover thermostat. In simulations based on the Martini force field, the target system temperatures were set to 240 K, 260 K, 280

K, 300 K, and 320 K, respectively, with a time step of 20 fs. In simulations based on the OPLS-UA force field, the target temperatures were 280 K, 290 K, 300 K, 310 K, and 320 K, respectively.

(*shown in lines 49 ~ 77, pages 3-4 in the supplement file*)

Fig. S2 presents an example of energy-tracking analysis, recording the time-evolution of interaction energy between water molecular clusters and dodecane clusters ($E_{w\text{-}d}$) for the 2000 dodecane – 8000 water system at 280 K based on the OPLS-UA force field. The system is considered to have attained equilibrium once the energy profile converges to an approximate stable value. Following equilibration, atomic-position trajectories were sampled statistically every 2 ps over a total simulation duration of 3 ns.

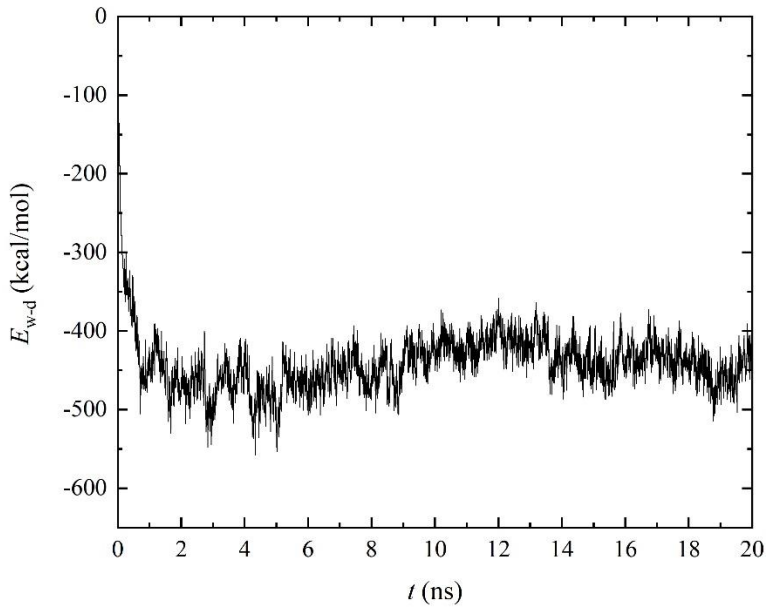


Fig. S2 The interaction energy between the water cluster and the dodecane cluster ($E_{w\text{-}d}$) in the LLPS droplet consisted of 2000 dodecane and 8000 water at the temperature of 280 K, and the MD simulation is based on the OPLS-UA force field

(*shown in lines 71 ~ 81 , page 4 in the supplement file*)

II.2) The geometrical contact angle retrieval method used in this manuscript heavily relies on the assumption that the droplets assume a spherical cap geometry, which is known to be false for droplets with radii inferior to 7 nm, as the amplitude of capillary wave fluctuations that perturb all fluid interfaces becomes comparable to the droplet radius below such cutoff diameters. Please present the temporal evolution of a sphericity metric for both partial droplets to justify the validity of the spherical cap approximation.

Answer: Thank you very much for this valuable comment. According to the reviewer's suggestion, we calculated the sphericity for both partial droplets. The added content is as follows.

The sphericity metric of the droplet (S_{fit}) is quantified based on the residual error from density profile fitting, consistent with the interface detection workflow adopted for contact angle calculation in this work. S_{fit} is given by

$$S_{fit} = 1 - \frac{\delta_{RMS}}{R_{fit}} \tag{3}$$

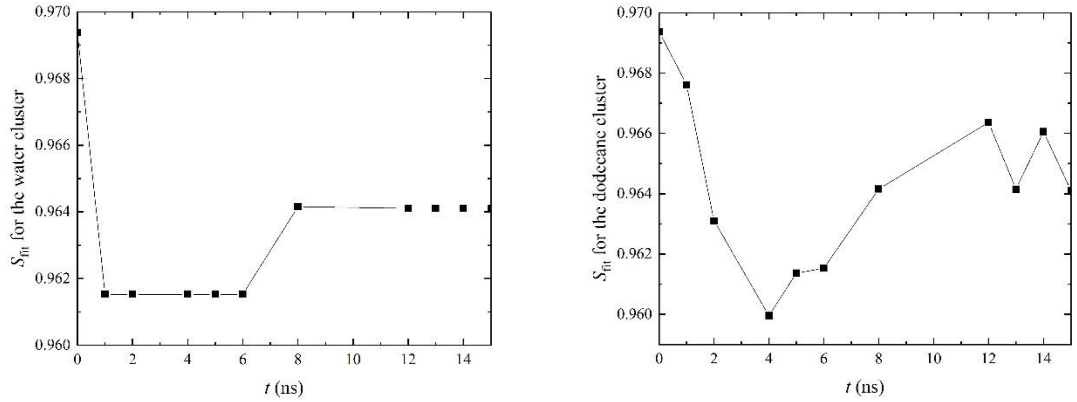
where δ_{RMS} is the Root mean square deviation of the distance from the interface point to the fitted sphere. R_{fit} is the optimal sphere radius obtained by least squares fitting. The δ_{RMS} is calculated by

$$\delta_{RMS} = \sqrt{\frac{1}{N_j}\sum_j (R_j - R_{fit})^2} \tag{4}$$

where R_j is the distance from each interface point to the centroid.

The temporal evolutions of S_{fit} for the water cluster and the dodecane cluster in the 2000 dodecane – 8000 water system at T = 280 K have been calculated, and the results are shown in Fig. S3. It can be easily found that the sphericity decreases first and then increases as the simulation progresses. At the initial stage, water clusters and dodecane clusters are ideal spherical shapes directly generated by software, therefore their sphericity is relatively high. With the evolution of the simulation, structural relaxation of the two clusters causes an initial reduction and subsequent rise in sphericity, with both clusters attaining near-equilibrium at approximately 8 ns. At equilibrium, the sphericity of both clusters is greater than 0.963, which proves the reliability of the assumption of spherical caps in calculating contact angles. At equilibrium, the

sphericity of both clusters is greater than 0.963, which proves the reliability of the assumption of cluster sphericity in calculating contact angles.



(a) (b)

Fig. S3 Temporal evolutions of S_{fit} for the water cluster (a) and the dodecane cluster (b) in the 2000 dodecane – 8000 water system at T = 280 K

(***shown in lines 82 ~ 106 , pages 4-5 in the supplement file***)

II.3) Depending on how the systems were prepared, sessile droplet-style contact angle simulations can be easily trapped in metastable states (e.g. when water droplets on solid surfaces are initiated from a cubic water slab or perfectly spherical droplet is placed on top of the surface). The theoretically correct way to prepare such systems is to allow the two phases to collide and assume their equilibrium shape within the simulation. State how the systems were prepared and how thermodynamic equilibrium was ensured. Present (at least in supporting information) the time evolution of the droplet morphology (contact angle) at least for the slowest evolving system (likely the largest number of atoms with the lowest temperature)

Answer: Thank you very much for this valuable comment.

The methods for establishing the model and confirming system balance are as follows.

Moltemplate was used to establish the initial droplet models. The initial configuration contained two tangential clusters: one cluster was water (or water mixed

with sodium chloride or suberic acid), and the other was pure dodecane. The system firstly underwent pre-equilibration for 2 ns at 240 K, then was heated to the target temperature for subsequent equilibrium runs. The interaction energy between the two clusters was monitored to assess whether the system reached equilibrium during pre-equilibration.

(*shown in lines 49 ~ 55 , page 3 in the supplement file*)

Fig. S2 presents an example of energy-tracking analysis, recording the time-evolution of interaction energy between water molecular clusters and dodecane clusters ($E_{w\text{-}d}$) for the 2000 dodecane – 8000 water system at 280 K based on the OPLS-UA force field. The system is considered to have attained equilibrium once the energy profile converges to an approximate stable value. Following equilibration, atomic-position trajectories were sampled statistically every 2 ps over a total simulation duration of 3 ns.

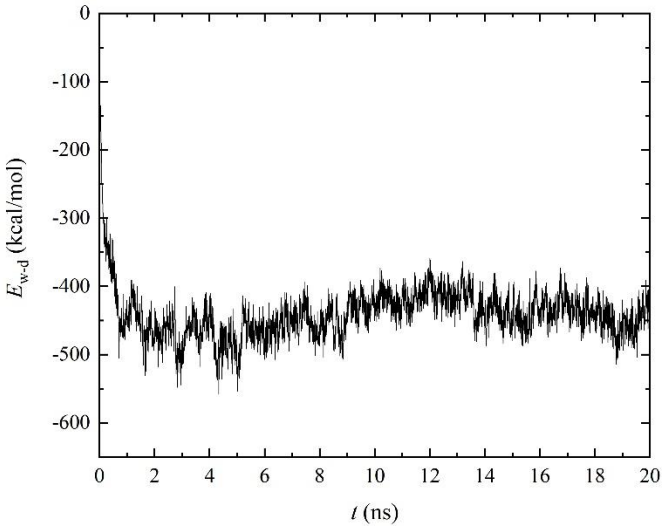


Fig. S2 The interaction energy between the water cluster and the dodecane cluster ($E_{w\text{-}d}$) in the LLPS droplet consisted of 2000 dodecane and 16000 water at the temperature of 300 K, and the MD simulation is based on the OPLS-UA force field

(*shown in lines 71 ~ 81 , page 4 in the supplement file*)

The time evolution of the contact angle in the 2000 dodecane – 8000 water system at T = 280 K is shown in Fig. S4

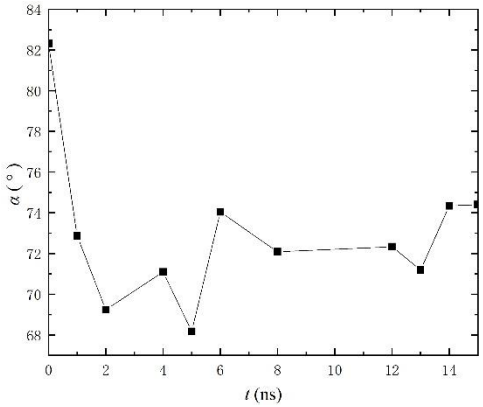


Fig. S4 Temporal evolution of the contact angle in the 2000 dodecane – 8000 water system at T = 280 K

II.4) Please comment on how relevant the chosen particle size (up to 20 nm) for real atmospheric particles is.

Answer: Thank you very much for this valuable comment. We summarize the key relevance points and manuscript revisions below:

(1) The 5–20 nm size range covers nucleation-mode nanoparticles abundant in urban and rural troposphere, formed via combustion emissions and new particle formation; these particles dominate total aerosol number concentration and represent the early growth stage of LLPS secondary aerosols containing nonpolar organics (dodecane proxy) and aqueous inorganic phases.

(2) No current laboratory technique can quantitatively measure liquid-liquid contact angles for particles <50 nm, so our MD data fills a critical missing dataset for nanoscale LLPS thermodynamics inaccessible to observation.

We acknowledge that most aged LLPS aerosols exceed 20 nm, and we have added clear text in the Conclusions to restrict our interpretations to fresh ultrafine particles below 20 nm, with future work on larger particles proposed.

It should be acknowledged that our model systems are simplified compared to real multi-organic multi-salt atmospheric aerosols. All simulated LLPS droplets are smaller than 20 nm, representative of fresh nucleation mode ultrafine particles from new particle formation and fuel combustion. Though these nanoparticles dominate ambient aerosol number concentrations and govern early aging processes, our results cannot be directly extrapolated to larger aged accumulation mode aerosols. Future simulations will cover more complex multicomponent mixtures and a wider particle size range.

(***shown in lines 648 ~ 654 , page 36 in the revised manuscript***)

II.5) In Section 3.4 the authors state that water-organic interface is « a plate ». Can you support this statement by snapshots from the simulations zooming on the interfacial zone?

Answer: We thank the reviewer for this careful question regarding our analogy of the water (-NaCl) cluster as a "plate". We hereby clarify the core meaning of this analogy to eliminate potential misunderstanding:

This wording does not indicate that the water (-NaCl)-dodecane interface is geometrically flat. Instead, the entire spherical water (-NaCl) cluster is merely regarded as a substrate, which is only mathematically analogous to the rigid solid substrate used in the classic Young's equation framework. This theoretical formulation was originally put forward by Fletcher (1958) for systems with convex spherical substrates, and has been broadly adopted in previous molecular dynamics simulations of liquid-liquid phase separated aerosols (Qiu and Molinero, 2015), which we follow throughout this work.

II.6) Comparison of the simulated surface tensions (Figure 8) with earlier MD-data obtained with identical potentials is not necessary. It could be moved to the SI as consistency check, if the authors wish to present it.

Answer: We appreciate this constructive suggestion. After careful consideration, we prefer to retain Figure 8 in the main text rather than shifting it to the supplementary information, for two key reasons:

First, the interfacial-tension values shown in Figure 8 serve as the core input parameters for the subsequent Young's equation evaluation in Section 3.4. The comparison between direct MD simulated contact angles and those predicted from Young's equation (Figure 9) entirely builds upon these interfacial tension results. Moving Figure 8 to the Supplement would break the logical chain in the main manuscript and force readers to repeatedly jump between the main text and supplementary material to follow the analysis of Young's equation applicability at the nanoscale.

Second, alongside previous MD results from identical force fields, Figure 8 includes experimental interfacial-tension benchmarks. Directly contrasting our simulated interfacial tensions against experimental measurements in the main text provides critical validation for the reliability of our Martini and OPLS-UA simulation setups. This experimental comparison strengthens the credibility of our subsequent contact angle and line-tension analyses, which constitute the central findings of this work.

III. Editorial comments:

III.1) line 117: were consisted —> consisted

Answer: Thank you very much for this valuable comment. The revisions incorporated in the revised manuscript are listed below.

The binary droplets were consisted of 2000 dodecane molecules and different numbers of water molecules

is revised to

The binary droplets consisted of 2000 dodecane molecules and different numbers of water molecules

(***shown in lines 118 ~ 119 , page 6 in the revised manuscript***)

III.2) line 202: under the same temperature condition would read better as at the

same temperature.

Answer: Thank you very much for this valuable comment. The revisions incorporated in the revised manuscript are listed below.

Under the same temperature condition, as the water content increases, the size of the water clusters increases, and the liquid-liquid contact angle shows a tendency to increase.

is revised to

At the same temperature, as the water content increases, the size of the water clusters increases, and the liquid-liquid contact angle shows a tendency to increase.

(***shown in lines 213 ~ 215 , page 11 in the revised manuscript***)

III.3) line 206 mechanisms of temperature and water content would read better as effects/ impacts of temperature and water content.

Answer: Thank you very much for this valuable comment. The revisions incorporated in the revised manuscript are listed below.

Based on the qualitative description, we further studied the mechanisms of temperature and water content on the liquid-liquid contact angle of the water-dodecane binary droplet,

is revised to

Based on the qualitative description, we further studied the effects of temperature and water content on the liquid-liquid contact angle of the water-dodecane binary droplet,

(***shown in lines 217 ~219 , page 11 in the revised manuscript***)

III.4) line 232 is presented —> is present

Answer: Thank you very much for this valuable comment. The revisions incorporated in the revised manuscript are listed below.

It should be noted that NaCl is presented only in the water clusters.

is revised to

It should be noted that NaCl is only present within the water clusters.

(***shown in line 248, page 13 in the revised manuscript***)

III.5) line 250 mass centre —> centre of mass

Answer: Thank you very much for this valuable comment. The revisions incorporated in the revised manuscript are listed below.

distance between the mass center of the ellipsoidal water cluster and the dodecane cluster exhibit a significantly reduction

is revised to

distance between the centers of mass of the ellipsoidal water cluster and the dodecane cluster exhibits a significantly reduction

(***shown in lines 266 ~ 267 , page 15 in the revised manuscript***)

III.6.) In the left panel of Figure 6 the periodic image of the aqueous droplet clearly comes from incorrect treatment of periodic boundaries by the visualisation software and should be removed.

Answer: We appreciate the reviewer's careful observation of Figure 6. We respectfully clarify that the separate aqueous droplet panel on the left is not a periodic boundary artifact, but a purpose-designed filtered view: we hid all dodecane molecules from the same trajectory frame to independently display the distribution of suberic acid within the aqueous phase, and periodic image replication was completely turned off during visualization. To resolve this misinterpretation, we have supplemented a detailed explanation in the Figure 6 caption to clarify the split panel visualization logic, and optimized the figure layout to better distinguish the full composite droplet and the water-suberic acid-only auxiliary view.

The small separated panel beside each main snapshot at the temperature of 280 K filters out all dodecane molecules to solely show water and suberic acid, for clear observation of suberic acid

interfacial distribution

(shown in lines 312 ~ 314 , page 17 in the revised manuscript)

III.7) line 519 adsorption coefficient —> absorption coefficient.

Answer: Thank you very much for this valuable comment. Your modification has made us realize that changing the adsorption coefficient to an accomodation coefficient is better, as it can be consistent with the context. The revisions incorporated in the revised manuscript are listed below.

If the adsorption coefficient of each liquid phase in the liquid-liquid phase separation particles is known

is revised to

If the accommodation coefficient of each liquid phase in the liquid-liquid phase separation particles is known

(shown in lines 570 ~ 571 , page 32 in the revised manuscript)

References

Fletcher, N. H.: Size effect in heterogeneous nucleation, The Journal of chemical physics, 29, 572-576, 1958.

Iannetti, L., Cambiaso, S., and Rasera, D. T., Antonio: The surface tension of Martini 3 water mixtures, J. Chem. Phys., 161, 2024.

Jorgensen, W. L., Maxwell, D. S., and Tirado-Rives, J.: Development and testing of the OPLS all-atom force field on conformational energetics and properties of organic liquids, J. Am. Chem. Soc., 118, 11225-11236, 1996.

Kulmala, M., Vesala, T., and Wagner, P. E.: An analytical expression for the rate of binary condensational particle growth, Proceedings of the Royal Society of London. Series A: Mathematical and Physical Sciences, 589-605, 1993.

Marrink, S. J., Risselada, H. J., Yefimov, S., Tieleman, D. P., and De Vries, A. H.: The MARTINI force field: coarse grained model for biomolecular simulations, J. Phys. Chem. B, 111, 7812-7824, 2007.

Obeidat, A., Hrahsheh, F., and Wilemski, G.: Scattering Form Factors for Russian Doll Aerosol Droplet Models, J. Phys. Chem. B, 119, 9304-9311, 2015.

Qiu, Y. and Molinero, V.: Morphology of liquid–liquid phase separated aerosols, J. Am. Chem. Soc., 137, 10642-10651, 2015.

Souza, P. C., Alessandri, R., Barnoud, J., Thallmair, S., Faustino, I., Grünewald, F., Patmanidis, I., Abdizadeh, H., Bruininks, B. M., and Wassenaar, T. A.: Martini 3: a general purpose force field for coarse-grained molecular dynamics, Nat. Methods, 18, 382-388, 2021.